

# Fast $^1\text{H}$ Missing-Pulse SSFP Chemical Shift Imaging of the Human Brain at 7 Tesla

D. Mayer<sup>1</sup>, and D. M. Spielman<sup>1</sup>

<sup>1</sup>Radiology, Stanford University, Stanford, CA, United States

## Introduction

Recently, steady state free precession (SSFP) chemical shift imaging techniques have been introduced [1-4] which are particularly attractive because of their short measurement time ( $T_{\text{acq}}$ ) and high sensitivity ( $\text{SNR}/\sqrt{T_{\text{acq}}}$ ). The main disadvantages of SSFP-based methods are that the effects of both T1 and T2 on the signal intensities complicate quantitation and the spectral resolution is limited due to the short TRs. Whereas the former is an inherent problem, the latter is less problematic at high field strengths such as 7 T due to the increased dispersion of the chemical shift. Spectroscopic missing pulse SSFP (spMP-SSFP) [4] has the advantage that the full echo can be acquired. This allows data to be analyzed in magnitude mode without spectral line broadening. Therefore, the aim of this work was to implement spMP-SSFP with a spectral-spatial radiofrequency (RF) pulse for combined water and lipid suppression at 7 T.

## Methods

All measurements were performed on a GE 7 T MR scanner equipped with self-shielded gradients (40 mT/m, 150 mT/m/ms). A GE quadrature birdcage coil was used for both RF excitation and signal reception. The sequence was tested on phantoms and on healthy volunteers.

The basic scheme of the implemented spMP-SSFP sequence is depicted in Fig. 1a. A 12-ms spectral-spatial RF pulse designed with the SLR algorithm [5] was used for simultaneous slice selection along  $z$  and water/lipid suppression. The simulated frequency and spatial profile of the pulse (opposed null design) is shown in Fig. 1b. The slice thickness was 5 mm. For the phantom experiment,  $32 \times 32$  phase encoding steps in  $k_x$  and  $k_y$  (FOV = 24 cm) were carried out corresponding to a nominal resolution of  $0.3 \text{ cm}^3$ . For the in vivo experiment, the matrix size was  $16 \times 16$  ( $1.1 \text{ cm}^3$ ). The flip angle  $\alpha$  was  $45^\circ$ . With a pulse interval  $\tau = 61 \text{ ms}$ , TR was  $3\tau = 183 \text{ ms}$ . The acquisition time per TR was 102 ms (spectral width = 10 kHz). With 2 averages for the phantom and 8 averages for the in vivo experiment to increase the SNR, the total measurement time ( $T_{\text{meas}}$ ) was 6:26 min including 64 cycles without acquisition to establish a steady state.

Apodization of the 3D data sets comprised multiplication with a squared sine-bell filter in the time dimension and with a generalized Hamming filter ( $\alpha_{\text{Ham}} = 0.6$ ) in both spatial frequency dimensions. After zero-filling in  $k_z$  by (factor 4), a 3D-FFT was performed and magnitude spectra were calculated.

## Results and Discussion

A spectrum from a single voxel at the center of a spherical GE MRS phantom filled with a solution of various brain metabolites at physiological concentration levels is shown in Fig. 2. Although the acquisition time corresponds to a nominal spectral resolution of only 10 Hz, the signals from creatine (Cr) and choline containing compounds (Cho) were completely separated even in magnitude mode, owing to the increased frequency dispersion at 7 T and the symmetric acquisition of the echo in spMP-SSFP. N-acetyl-aspartate (NAA), *myo*-inositol (mI) and glutamate (Glu) could also be detected. Due to the severe  $B_1$  inhomogeneity of the RF coil used, the signal intensity varied considerably over the phantom ( $\sim 18\text{-cm}$  diameter). This signal variation can also be seen in the grid of spectra from a healthy volunteer (Fig. 3a). The selected slice was just superior to the ventricles and the location of the spectra is indicated in the corresponding MRI displayed in Fig. 3b. A spectrum from a single voxel is shown Fig. 3c. Similar to the phantom results, the signals from total Cr (tCr) and Cho are well separated. Although the depicted voxel was near the center of the brain, artifact signal from subcutaneous lipids in the scalp were detected because of incomplete suppression and Gibbs-ringing. Nevertheless, the NAA singlet at 2 ppm was not affected.

## Conclusion

The presented data demonstrate the advantages and current challenges of spMP-SSFP at 7 T. The higher field strength provides better signal separation and higher SNR relative to low- and mid-field systems. Even when using a relatively small flip angle ( $45^\circ$ ) with the currently available RF coil,  $B_1$  inhomogeneity has a substantial impact on data quality. Better coil designs and parallel RF transmission techniques should help to reduce the artifacts caused by  $B_1$  inhomogeneity. When signal averaging is necessary to increase the SNR, a 3D variant of the technique can be used alternatively without time penalty.

## Acknowledgement

This work was supported by NIH grants RR09784, AA12388, and AA13521.

## References

[1] Dreher W et al., Magn. Reson. Med. 50, 453-460 (2003). [2] Geppert C et al., MAGMA 19, 196-201, 2006. [3] Althaus M et al., Magn. Reson. Imag. 24, 549-555 (2006). [4] Schuster C et al., Proc. ISMRM 2006, 71. [5] Pauly J et al., IEEE Trans. Med. Imag. 10, 53-65 (1991).

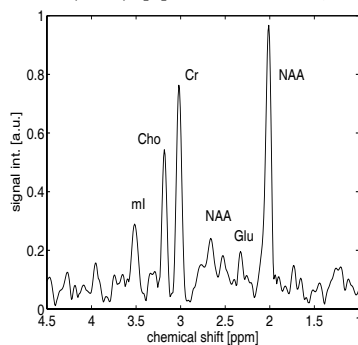


Fig. 1: Magnitude spectrum from a single voxel at the center of the phantom (nom. voxel size:  $0.3 \text{ cm}^3$ ,  $T_{\text{meas}} = 6:26 \text{ min}$ ).

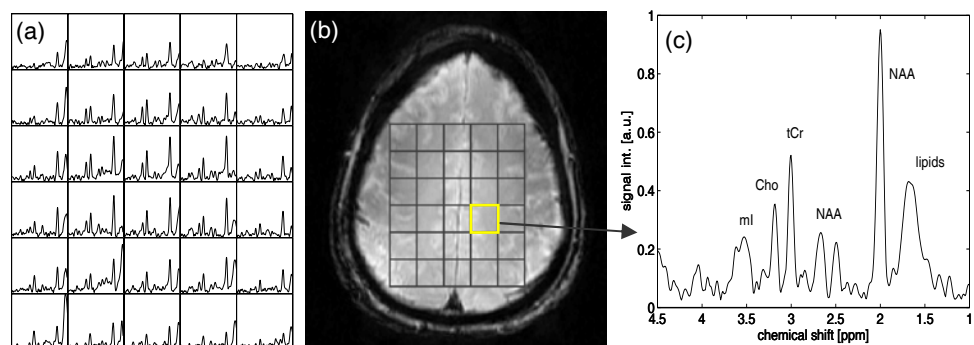


Fig. 3: (a) Magnitude spectra (4 ppm to 1.5 ppm) from a healthy volunteer. (b) Water GRE image overlaid by a grid indicating the location of the spectra in (a). (c) Magnitude spectrum from a central voxel of the data set (nom. voxel size:  $1.1 \text{ cm}^3$ ,  $T_{\text{meas}} = 6:26 \text{ min}$ ).

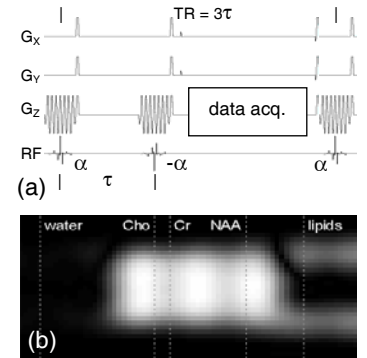


Fig. 1: (a) RF and gradient scheme of spMP-SSFP. (b) Simulated 2D profile of the spectral-spatial RF pulse.